

Figure 6.6.2 Meldorf Bay Test Case: Bathymetry

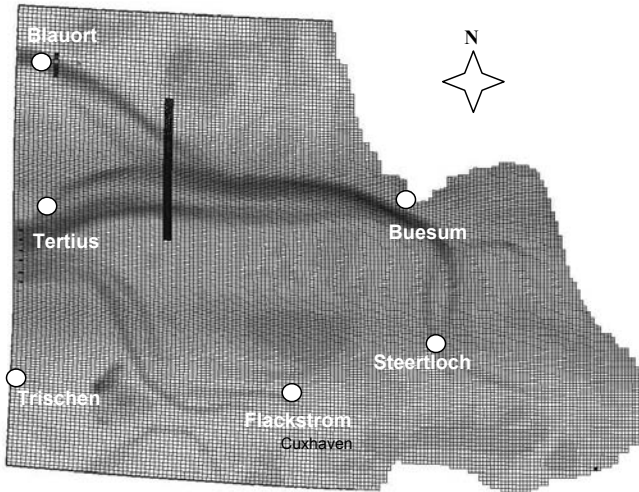


Figure 6.6.3 Meldorf Bay Test Case: Model grid and location of water level gauges

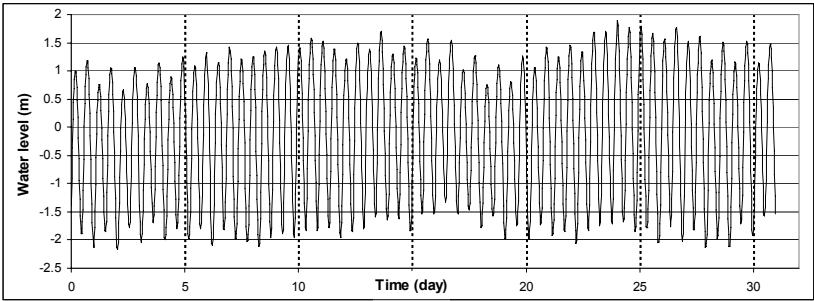


Figure 6.6.4 Meldorf Bay Test Case: Water level elevation at station Trischen, May 1990

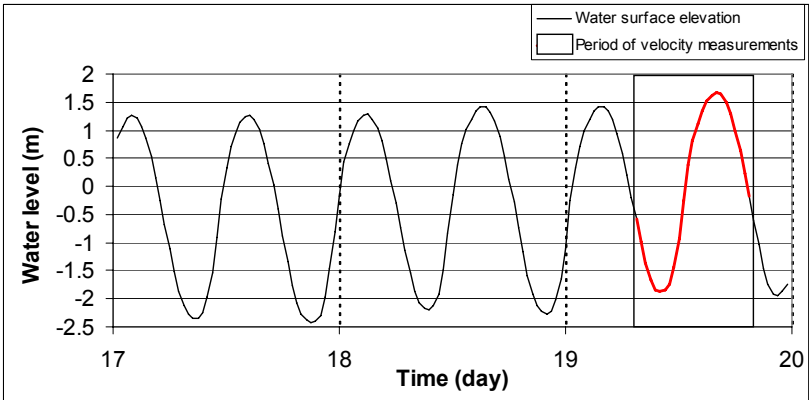


Figure 6.6.5 Meldorf Bay Test Case: Water level elevation and period of velocity measurements at station Tertius

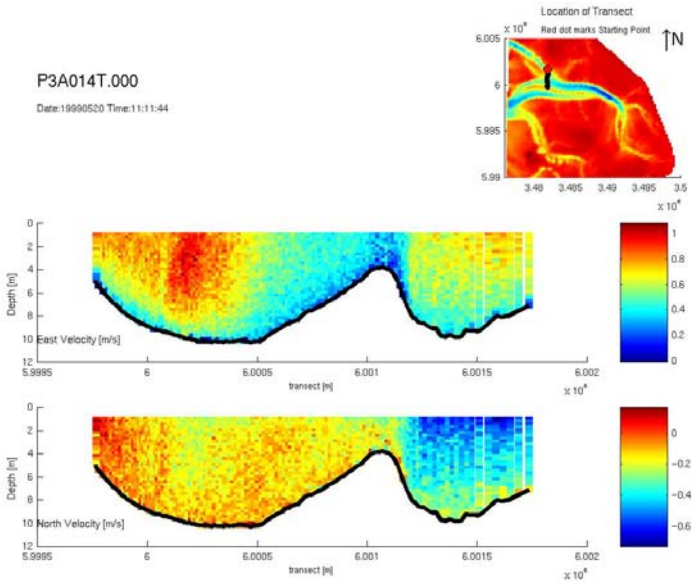


Figure 6.6.6 Meldorf Bay Test Case: Measured water velocities (May 20th 1999, 11:11)

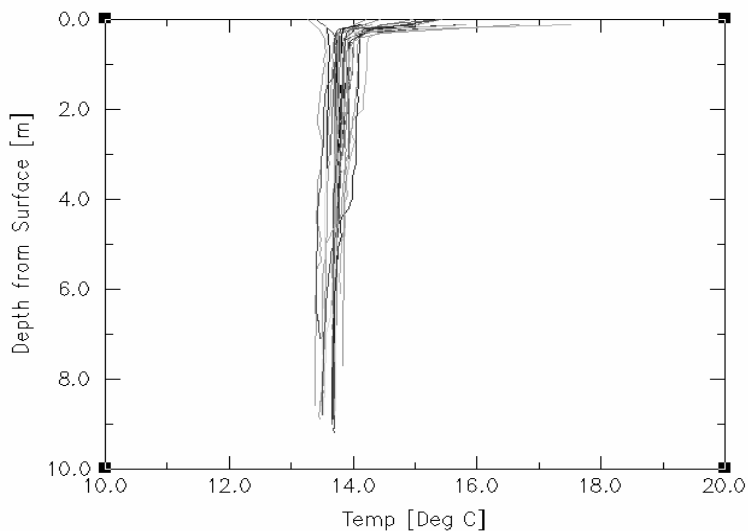


Figure 6.6.7 Meldorf Bay Test Case: Measured water temperature profiles for May 20th 1999

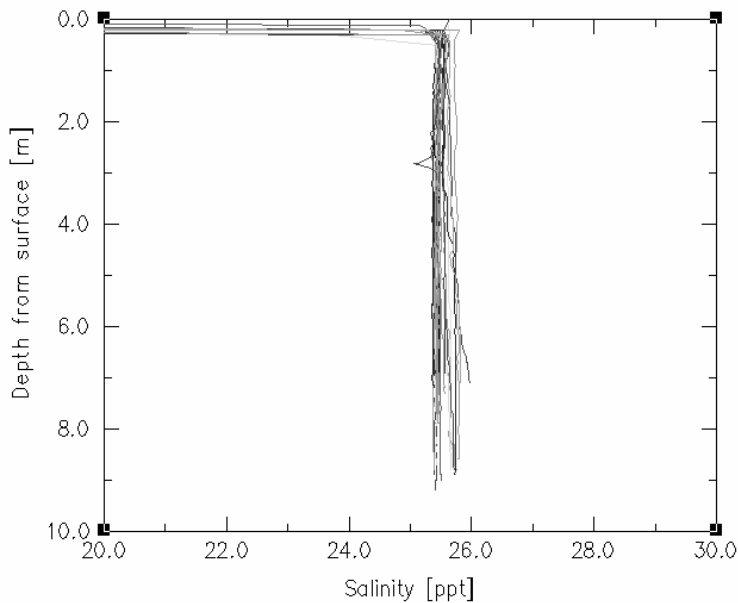


Figure 6.6.8 Meldorf Bay Test Case: Measured water salinity profiles for May 20th 1999

6.7 TOKYO BAY TEST CASE

Contributors: Mutsuto Kawahara, Toshio Kodama, and Yan Ding

6.7.1 Background

The simulation and prediction of three-dimensional flow in coastal areas are needed for planning navigation channel construction, designing harbor and offshore structures, assessing the environmental and ecological impacts of coastal engineering projects. This test case provides a set of comprehensive 3D tidal current measurements in Tokyo Bay taken during a period from 25 August to 25 October 1983. The database consists of the bathymetry of the bay, tidal levels at eight stations and currents measured at several locations as well as different water depths. In addition, it suggests the values of physical constants and boundary forcing conditions including incident tidal waves, river inflow velocities, and wind velocities above the water surface. Kodama et al. (1996) have conducted the hydrodynamic modeling of the 3D tidal current by utilizing this database. A multiple-level finite elemental model was validated in their studies by comparing the numerical results with the observed tidal current data. A series of numerical experiments were carried out to carefully examine the tidal circulations affected by the forcing factors of Coriolis force, river inflows and wind shear stresses, either individually or combined (Kodama et al. 1996).

The correct specification of tidal wave boundary conditions is of vital importance in modeling tidal flows in harbors, estuaries, and tidal rivers. The persistent difficulties in specifying the tidal waves at open boundary are mainly caused by two reasons. First, there may not be any measurements of water elevations at the specified open boundary. However, as long as water elevations and/or currents have been measured at some locations in the considered water region, the tidal waves at the specified open boundary can be estimated by means of optimal theories to minimize the discrepancies between simulations and observations in the region. In fact, parameter identification techniques have been widely used in the simulation of flood waves, ocean circulations, and tidal flows. Lardner (1993) presented a procedure for optimal control of open boundary conditions in a numerical tidal model. Gunson and Malanotte-Rizzoli (1996) then provided an optimal theory for identifying open boundary conditions and initial conditions in an open-ocean flow model. In the case of Tokyo Bay, using the linearized shallow water equations, Kodama and Kawahara (1992) proposed a procedure by means of an optimal theory to estimate the tidal waves at the open boundary. Then, Kodama et al. (1991) used the nonlinear shallow water equations to improve the estimated amplitudes of the incident tidal waves.

Second, because the incident wave trains will reflect on solid walls in the computational domain, if the open boundary does not permit the reflective waves to freely go out, the outgoing waves will reflect on the boundary toward the internal domain to generate spurious reflective waves (Kodama et al. 1991). Generally, the incident waves are continuous wave trains propagated from the deep-water region of sea; the reflective waves are generated from the internal domain including the open

boundary during wave reflections. The spurious reflective waves always destabilize the computation of the initial transient flow on the open boundary when the tidal flow starts from the static state (“cold start”), and predict the initial tidal flow with seriously non-physical oscillations, because the reflective waves introduce the modes of free oscillations in the computational domain (Blumberg and Kantha, 1985; Kodama and Kawahara, 1992). Directly specifying the water elevations cannot avoid this non-physical reflection at the boundary, in principle. The outgoing waves should freely transmit through the open boundary without the spurious reflections on the boundary. Therefore, it is necessary to distinguish between the incident waves and the reflective waves at the open boundary. The latter should be allowed to go out freely, in order to eliminate the spurious reflective waves (Kodama et al. 1991). This treatment, which is called “non-reflective open boundary condition”, is identical to the absorbing wavemaker in laboratory experiments of wave generations (Schaffer et al. 1994; Lin and Liu, 1999).

6.7.2 Objectives

This test case provides a database of field data consisting of tidal levels and tidal currents at a large number of measuring stations in and around simulation domain. It can be used to determine the 3D hydrodynamic model’s capability of predicting tidal processes. The following tidal processes generated by hydrodynamic model can be validated:

- How realistic are the predicted tidal levels during the observed period?
- Are the 3D currents and residual current structure simulated under incident tidal waves in reasonable agreement with those measured at several observation stations over a tidal cycle?

6.7.3 Approach

In general, before running a 3D tidal current model, users have to use the bathymetric data provided in the database to generate a 3D computational mesh. Then users need to define the boundaries in the computational domain, and impose the incident tidal waves and river inflows on the corresponding boundaries. Users also need to set up some of physical parameters to include other external forces in the model, e.g., the Coriolis force and wind shear stresses. All of the data about the bathymetry of the bay, incident tidal waves, and discharges of river inflows have been provided in this test case.

As an example for explaining the validation approach, a multiple-level finite element model proposed by Kawahara et al. (1983) and further modified by Kodama et al. (1996), is introduced as follows. Assuming the vertical acceleration of a large water body is negligible, and the hydrostatic pressure distribution is adopted, the three-dimensional computational domain can be idealized as a multiple-level domain. To do so, only a two-dimensional computation at each level is necessary. This model is general enough to include the effects of Coriolis force, river inflows and wind shear stresses. The non-reflective wave condition has been applied on the open boundary to

filter off spurious reflection waves. The density of water is treated as a constant in each level, but it may be different from other levels. To simulate 3D tidal currents, the following data have been already provided:

- Finite element mesh, nodal connections in vertical direction, different set of nodal points on boundaries for specifying incident tidal wave, river inflows, and coastal lines and/or river banks;
- Incident tidal wave conditions: Four major tidal constituents generated the incident tidal waves;
- Physical constants;
- Resistance coefficients of wind and bottom friction;
- River inflow velocities;
- Initial condition: cold start;
- Time increment: 15s for the multiple-leveled model;
- Selected nodal points and variables for outputs of numerical results: tidal levels at eight tide elevation gauges, and tidal currents at ten observation stations;
- Calculation of residual current: the computational period is six days in the multiple-leveled model; the tidal currents at final tidal period of M_2 were used to calculate the residual currents.

6.7.4 Physical Domain

Tokyo Bay shown in Figure 6.7.1 is about 48km long and 37km wide, located off the southeast coast of Honshu Island, Japan, connected to the West Pacific Ocean. It provides a spacious harbor area for several Japanese cities, including Tokyo and Yokohama. The three-dimensional tidal currents in the bay were measured during the period from 25 August to 25 October 1983. The measurements of the tidal currents were made to establish a fundamental database on flow profiles in the bay. Meanwhile, oceanographic and meteorological data such as tidal levels, wind, precipitation, atmospheric pressure, etc., have been collected at some observation points shown in Figure 6.7.1. During the observation period, there were totally ten observation stations for monitoring 3D tidal current, eight tide gauges for recording surface elevation, and others around the bay for measuring wind velocity, atmospheric pressure, river discharge, and precipitation (Yokohama, 1983). Mainly, four rivers (i.e. Edogawa River, Arakawa River, Tama River, and Tsurumi River) discharge freshwater into the bay. The water depth contours in Tokyo Bay are shown in Figure 6.7.2 (Maritime Safety Agency, 1984). The locations of the tide gauges and the observation stations of tidal currents in a triangular mesh of surface level in the multiple-level finite elemental model are indicated in Figure 6.7.3.

6.7.5 Numerical Grid and Bathymetry

Kodama et al. (1996) have applied a multiple-level finite element model to simulate the tidal currents during the observation period in Tokyo Bay. The triangular finite element meshes of Tokyo Bay shown in Figure 6.7.3 (surface mesh only) and Figure

6.7.4 (meshes in five different levels) has been employed. In the surface mesh system, the total numbers of nodes and elements at the surface level are 685 and 1216 respectively. The numerical meshes for the multiple-level finite element model at other levels are the projections of the surface triangular mesh. The water depth in the first layer between the first level and second level is 5m; the water depth of the other layers is 10m. Users can directly utilize this mesh system as their computational mesh, of which the digital data can be found in the file MESH.DAT in Appendix A of this report. The data showing the connection of nodal points and triangular elements between two adjacent levels are stored in the files NOD_CONK.DAT and ELE_CONK.DAT. The other information about the total nodal number and triangular element number can be found in the file LEVEL.DAT. All of these data files are given in Appendix A. In case of testing a fully three-dimensional model for tidal flows, users are advised to utilize the mesh data to generate their own three-dimensional mesh. In addition, users can use the surface mesh data in the file SURF_MESH.DAT that consists of water depth measured from the mean water level and wind velocities at nodal points of the surface triangular mesh.

6.7.6 Initial Conditions

The physical constants are listed in Table 6.7.1, including the air density, the Coriolis parameter, the horizontal eddy viscosity coefficient, the friction coefficients at the water bottom and the interfaces between two levels, and the profile of water density along vertical levels (The water density is assumed to be constant at each level). The static state of water body is used as the initial conditions (cold start), i.e., the initial water elevation is the static horizontal plane relative to the mean sea level.

Table 6.7.1 Physical constants in the multiple-level model

Wind drag coefficient	0.00015
Air density (kg/m^3)	1.29
Friction coefficient at interface	0.001
Friction coefficient at bottom	0.0026
Horizontal eddy viscosity coefficient (m^2/s)	10.0
Coriolis parameter	0.000084
Water density profile (from surface layer) (kg/m^3)	1010.0, 1015.0, 1020.0, 1025.0, 1030.0

6.7.7 Boundary Conditions

Incident Tidal Wave

In the test case, the incident tidal waves are imposed on the entrance (open boundary) of the bay (Figure 6.7.3). They consist of the four major tidal constituents, i.e., M_2 , S_2 , K_1 , and O_1 . The amplitudes of the four tidal constituents have been estimated by means of an identification method, by which a non-reflective boundary condition was imposed on the open boundary (Kodama et al. 1991). Using these incident tidal

waves, the multiple-level tidal model has generated the optimal tidal levels in excellent agreement with the observed tidal levels. The superposition of the incident tidal waves is represented as follows:

$$\eta(t) = \sum_{m=1}^4 a_m \sin \left[\frac{2\pi}{T_m} (t - t_0) - \phi_m \right], \quad (6.7.1)$$

where $\eta(t)$ means the observed tidal level at the time t ; t_0 is an initial time, equal to 0.0hr; for each tidal constituent, a_m , T_m , and ϕ_m are its tidal amplitude, tidal period, and phase delay, respectively. The amplitudes, periods, and phase delays of the four tides are listed in Table 6.7.2. Users can find the data in the file TABLE78.XLS. A set of nodal points relative to the location of the open boundary has been retrieved from the suggested mesh, and they can be found in the file NOD_OPNBC.DAT. If users choose the finite element mesh provided in the case as their computational mesh, they might directly impose the tidal wave on the open boundary.

Table 6.7.2 Tidal constituents of incident waves

Constituents	Amplitude a_m (m)	Period T_m (hour)	Phase delay ϕ_m (Rad)
M ₂	0.21	12.42	-5.8398
S ₂	0.15	12.00	-5.6018
K ₁	0.14	23.93	-1.3290
O ₁	0.10	25.82	-1.3211

For specification of tidal waves in the open boundary (Figure 6.7.3), users may choose one of the following two approaches. To avoid the complicated treatment of non-reflective boundary condition as proposed by Kodama et al. (1996), the simple approach is to directly specify the water elevations on the open boundary. The time series data of water elevations during 12 days at the open boundary can be found in the file OUTLET_WL.DAT, which are the computed water elevation at the middle point of the entrance of the bay by the multiple-level model (Kodama et al. 1996). The water elevations are the tidal levels on the open boundary considering both incident tidal waves and reflective waves. In order to eliminate the spurious reflective wave on the open boundary, the user may use a modified form of Sommerfeld radiation boundary condition, and refer to Blumberg and Kantha (1985) for details.

The second approach for specification of the open boundary condition is to impose a non-reflective boundary condition. Note that the incident waves have been identified from optimal estimation of predictive errors through taking account of the reflective waves generated from solid boundaries in the computational domain (Kodama et al. 1991; Kodama and Kawahara, 1992); the sum of the four major constituents is only the part of incident waves at the open boundary, not the total water elevation in the boundary. Therefore, since the water elevation at the open boundary consists of the incident wave and the reflective wave, the reflective wave in the boundary should be

calculated by considering the reflection on the internal boundaries due to the attack of incident waves. The calculation of reflective waves can be carried out in the simulation process. Detailed treatment about the reflective wave can be found in Kodama et al. (1996).

Due to the complexity in the approach of Kodama et al. (1996), we introduce a relatively simple way to estimate the reflective wave on the open boundary. It is assumed that water elevation on open boundary can be expressed as a linear combination of the incident and reflective wave:

$$\eta(n_0, t) = \eta^I(n_0, t) + \eta^R(n_0, t), \quad (6.7.2)$$

where $\eta(n_0, t)$ denotes the water elevation on the open boundary; n_0 is the normal direction at the boundary inward to the domain, η^I and η^R are the incident wave and the reflective wave components, respectively. The reflective wave at the adjacent node $n_0 + \Delta n$ in the internal domain can be calculated as follows:

$$\eta^R(n_0 + \Delta n, t) = \eta(n_0 + \Delta n, t) - \eta^*(n_0 + \Delta n, t), \quad (6.7.3)$$

where $\eta(n_0 + \Delta n, t)$ is the computed water elevation at the adjacent node including reflective waves; $\eta^*(n_0 + \Delta n, t)$ denotes water elevation at the adjacent node in the case where the incident wave goes through the node without reflective wave. For linear wave, it can be calculated as follows:

$$\eta^*(n_0 + \Delta n, t) = \sum_{m=1}^M a_m \sin\left(\frac{2\pi}{T_m} t - k_m \Delta n + \phi_m\right), \quad (6.7.4)$$

where M denotes the total number of tidal constituents, ϕ_m is the phase lag, k_m represents the wave number, i.e.,

$$k_m = \frac{2\pi}{T_m C}, \quad (6.7.5)$$

where $C = \sqrt{gh}$ is the wave velocity, and h is water depth at the open boundary. Then, the reflective wave component $\eta^R(n_0, t)$ at the open boundary can be computed by using the radiation condition,

$$\frac{\partial \eta^R}{\partial t} - C_r \frac{\partial \eta^R}{\partial n} = 0, \quad (6.7.6)$$

where C_r is the wave velocity of reflective wave, equal to C under the assumption of shallow water. This equation can be solved simply by means of a finite difference formulation in a subdomain near the open boundary by considering the reflective